

Article

Direct Synthesis of Ti-Containing CFI-Type Extra-Large-Pore Zeolites in the Presence of Fluorides

Yichen Wang¹, Hongjuan Wang¹, Yuanchao Shao¹, Tianduo Li^{1,*}, Takashi Tatsumi² and Jin-Gui Wang^{1,*}

¹ Shandong Provincial Key Laboratory of Molecular Engineering, School of Chemistry and Pharmaceutical Engineering, Qilu University of Technology (Shandong Academy of Sciences), Jinan 250353, China; wangyc610@163.com (Y.W.); hongjuanwang2015@163.com (H.W.); sychao629@163.com (Y.S.)

² Institute of Innovative Research, Tokyo Institute of Technology, 4259 Nagatsuta, Midori-ku, Yokohama 226-8503, Japan; tacchan.tatsumi@gmail.com

* Correspondence: ylpt6296@vip.163.com (T.L.); JGWang@qlu.edu.cn (J.-G.W.); Tel.: +86-531-89631208 (T.L.); +86-531-89631212 (J.-G.W.)

Received: 18 February 2019; Accepted: 12 March 2019; Published: 14 March 2019



Abstract: Ti-containing zeolites showed extremely high activity and selectivity in numerous friendly environmental oxidation reactions with hydrogen peroxide as a green oxidant. It will be in high demand to synthesize Ti-containing crystalline extra-large-pore zeolites due to the severe restrictions of medium-pore and/or large-pore zeolites for bulky reactant oxidations. However, the direct synthesis of extra-large-pore Ti-zeolites was still challengeable. Here, we firstly report a strategy to directly synthesize high-performance Ti-containing CFI-type extra-large-pore (Ti-CFI) zeolites assisted with fluorides. The well-crystallized Ti-CFI zeolites with framework titanium species could be synthesized in the hydrofluoric acid system with seed or in the ammonium fluoride system without seed, which showed higher catalytic activity for cyclohexene oxidation than that synthesized from the traditional LiOH system.

Keywords: Ti-CFI; Ti-CIT-5; extra-large-pore; zeolites; fluorides; titanosilicates; oxidation

1. Introduction

Zeolite, a type of crystalline microporous aluminosilicate, has wide applications in adsorption, separation, and catalysis, especially in oil refining and producing petrochemicals as solid-acid catalysts [1–6]. Incorporation of isolated titanium ions into a high-silica zeolite to achieve a Ti-containing zeolite, called titanosilicate, was a milestone in zeolites and heterocatalysis due to its extremely high activity and selectivity in numerous friendly environmental oxidation reactions with hydrogen peroxide as a green oxidant [7]. The discovered MFI-type and MWW-type zeolites were successfully applied in the industrial processes of the hydroxylation of phenol, the ammoximation of cyclohexanone/butanone, and the liquid-phase epoxidation of propylene to propylene oxide [8–11].

Subsequently, a series of Ti-containing zeolites with different topologies were synthesized including 10-ring medium-micropore (~0.55 nm in diameter) [12–14] and 12-ring large-micropore (~0.75 nm in diameter) zeolites [15–21]. However, considering the severe restrictions for the oxidation of bulky reactants in these 10-ring and 12-ring micropores, it would be in high demand to synthesize Ti-containing three-dimensionally crystalline extra-large-pore (larger than 12 rings) zeolites.

It was very difficult to directly crystallize the starting gel (containing silicon source, titanium source, and structure-directing agents) to form Ti-containing extra-large-pore zeolites because the titanium ion proved no structure-directing ability and its ionic radius was larger than that of the silicon ion, which led to difficulties in the crystallization of raw materials and the incorporation of

titanium into the zeolite framework [22,23]. Until now, only a few Ti-containing extra-large-pore zeolites were directly synthesized, including aluminophosphate (Ti-VPI-5) with an 18-ring [24], Ti-UTL with a 14-ring extra-large pore [25], Ti-UTD-1 (DON-type) with a 14-ring extra-large pore [26], and Ti-CIT-5 with a 14-ring extra-large pore [27]. So as to crystallize the raw materials, special and expensive structure-directing agents, i.e., bis(pentamethyl-cyclopentadienyl)cobalt(III) hydroxide for Ti-UTD-1 and lithium hydroxide as an accelerator for Ti-CIT-5 were required. However, the accelerator of lithium hydroxide for the crystallization of Ti-CIT-5 resulted in large amounts of extra-framework titanium species. For activating this extra-large-pore catalyst, further post-treatment processes were required. Therefore, effective strategies to prepare Ti-containing extra-large-pore zeolites were still desirable and significant.

Here, we firstly report a strategy to directly synthesize the high-performance Ti-containing CFI-type extra-large-pore (Ti-CFI) zeolites in the presence of fluorides. The influence factors such as the type of fluoride source, water content, and the additive of seed for the crystallization of Ti-CFI were investigated. The well-crystallized Ti-CFI zeolites with framework titanium species could be synthesized in the HF system with seed or in the NH_4F system without seed, which both showed higher catalytic activity for cyclohexene oxidation than that synthesized from the LiOH system.

2. Results and Discussion

2.1. Zeolite Characterization

Powder X-ray diffraction (PXRD) patterns (Figure 1) showed that Ti-containing CFI-type extra-large-pore zeolites could crystallize in the presence of fluorides. The crystallinity was very low after a 13-day crystallization if hydrofluoric acid was used as the fluoride source (Figure 1a), suggesting some amorphous materials present in the sample. When the concentration of the raw materials increased by decreasing the water content in the raw materials, the crystallinity was slightly increased as indicated by the increased diffraction intensity in Figure 1b. However, crystallinity was still very slow. The broad peak around $20\text{--}25^\circ$ implied the presence of amorphous raw materials in this sample. This indicated that well-crystallized Ti-CFI was difficult to achieve when hydrofluoric acid was used as a fluoride source, although pure silica CFI-type zeolite could be fully crystallized in the HF system (Figure S1, Supplementary Materials). This was also evidence that the synthesis of titanium-containing zeolite was more difficult than synthesis of Ti-free pure silica zeolite. If ammonium fluoride was employed as a fluoride source, as shown in Figure 1c, a sample with good crystallinity could be achieved after a 13-day crystallization. Moreover, all the peaks were consistent with the reported CFI-type topology [27], indicating as-synthesized zeolite without other impure phases. The addition of pure silica CFI-type seeds could accelerate the crystallization process, leading to the formation of a well-crystallized sample even within seven days, as indicated in Figure 1d.

SEM images indicated the presence of amorphous raw materials among the rod-like large crystals of Ti-CIT-5[HF]-13d synthesized in the HF system without seeds, which was consistent with the low diffraction intensity as shown in the PXRD pattern. Samples of Ti-CFI[NH_4F]-13d from the ammonium fluoride system possessed a rod-like crystalline shape with tens of micrometers in length as indicated in Figure 2b. Moreover, the crystal was large and was composed of the small rods. Interestingly, plate-like crystals with $5\text{--}10\ \mu\text{m}$ in length, $1\text{--}2\ \mu\text{m}$ in width, and $0.2\text{--}0.4\ \mu\text{m}$ in thickness could be formed if the seeds were added. No amorphous raw materials or other impure particles were found in the sample of Ti-CFI[HF]-seed-13d. Moreover, the crystal size was smaller than the samples synthesized with only HF and NH_4F , suggesting the role of the seed in accelerating the crystallization rate and decreasing the crystal size.

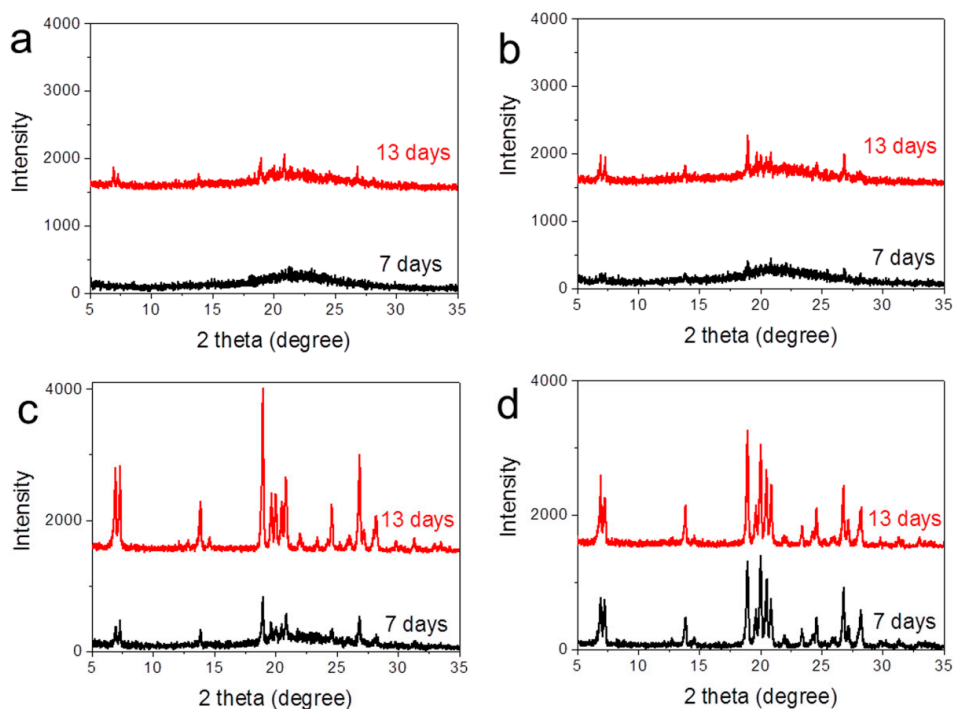


Figure 1. Powder X-ray diffraction (PXRD) patterns of extra-large-pore Ti-CFI zeolites synthesized under different conditions with different crystallization time. (a) Ti-CFI[HF] synthesized using hydrofluoric acid as a fluoride source; (b) Ti-CFI[HF]-L synthesized by decreasing the water content from 20 to 5 in the $\text{H}_2\text{O}/\text{SiO}_2$ molar ratio in the HF system; (c) Ti-CFI[NH_4F] using ammonium fluoride as a fluoride source; (d) Ti-CFI[HF]-seed by adding pure silica CFI-type zeolite as seeds in the HF system.

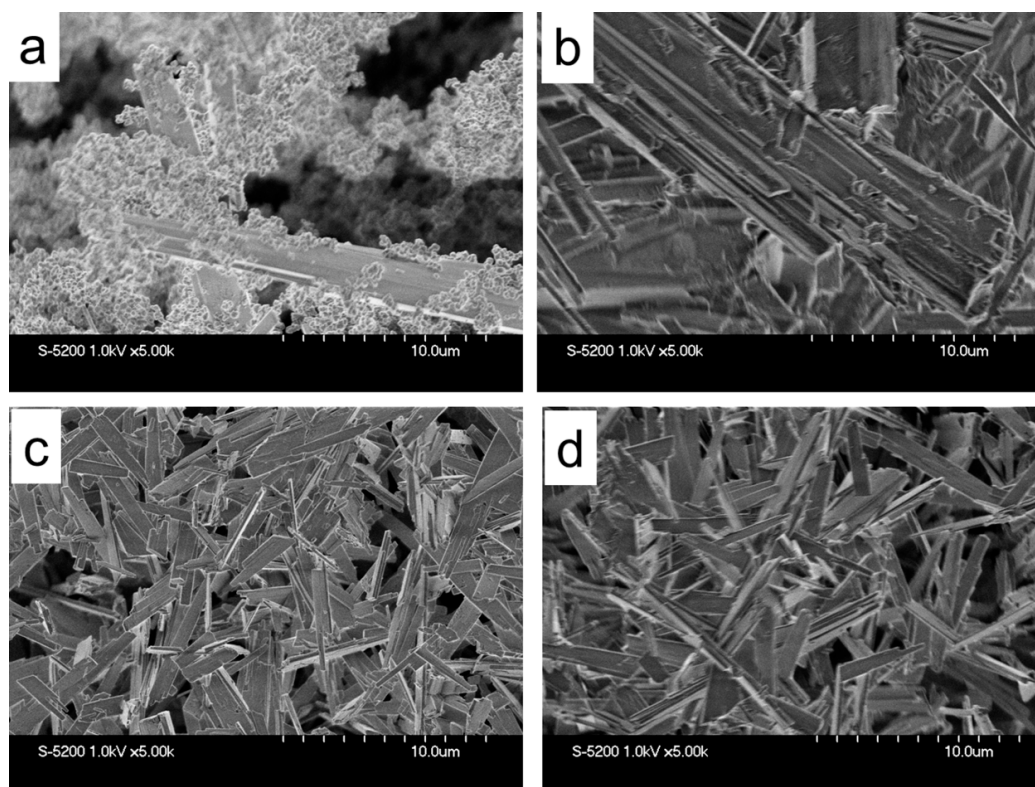


Figure 2. SEM images of (a) Ti-CIT-5[HF]-13d, (b) Ti-CFI[NH_4F]-13d, (c) Ti-CFI[HF]-seed-7d, and (d) Ti-CFI[HF]-seed-13d.

Nitrogen adsorption characterization showed that all the samples synthesized in the presence of fluorides had $\sim 400 \text{ m}^2 \cdot \text{g}^{-1}$ specific surface area. Comparing Ti-CFI[HF]-seed-13d and Ti-CFI[NH₄F]-13d, samples of seed-assisted synthesis in the HF system showed higher specific surface area, micropore volume, and external surface area than those of samples from the NH₄F synthetic system. The higher external surface area implied a small crystal size, which was consistent with the abovementioned SEM characterization. Comparing Ti-CFI[HF]-seed-7d and Ti-CFI[HF]-seed-13d, the long-time crystallization led to a slight increase in specific surface area and micropore volume. Meanwhile, the Ti content was effectively increased after long-time crystallization. Unlike the fluoride system, Ti-CFI[LiOH], which was directly synthesized from the LiOH system without further post-treatment, showed extremely low Brunauer–Emmett–Teller (BET) specific surface area and micropore volume. Post-treatment by washing with acid significantly increased the BET specific surface area and micropore volume of Ti-CFI[LiOH]-post, but decreased the Ti content. In addition, Ti-CFI synthesized in the presence of fluorides always showed a higher pore volume and lower external specific surface area than those of samples synthesized in the presence of LiOH. The larger amounts of external specific surface suggested a smaller crystal size of samples synthesized in the presence of LiOH (Figure S2, Supplementary Materials).

Titanium was the catalytic center in the Ti-containing zeolite for the epoxidation of olefins, which is of great important processes for producing fine chemicals. The state of Ti would greatly affect the catalytic performance. There are several types of Ti species in the presence of the zeolite, including tetrahedral coordinated and octahedral coordinated titanium species, and anatase-like TiO₂ tiny particles. Furthermore, it was proven that only tetrahedral (framework) Ti showed catalytic performance for the selective oxidation of olefins. The presence of octahedral (extra-framework) Ti and tiny TiO₂ particles would adversely affect the catalytic activity and decrease the utilization efficiency of hydrogen peroxide. Diffuse reflectance ultraviolet/visible light (UV/Vis) (DRUV/Vis) spectroscopy is an effective technique to detect the coordination states of Ti species. The absorbance peak at about 210 nm attributed to Ti⁴⁺O²⁻ → Ti³⁺O⁻ ligand-to-metal charge transfer was assigned to the framework Ti species. The broad absorbance peak at about 250 nm was assigned to the extra-framework Ti species. The peak at about 330 nm was assigned to the formation of tiny anatase-like TiO₂ particles [7]. As indicated in the Figure 3A, all the samples synthesized in the fluoride system showed the main band at about 210 nm, indicating that most of the titanium was present as framework Ti species. The presence of a shoulder peak at 250 nm indicated the presence of small amounts of extra-framework Ti species in these samples. In addition, Ti-CFI[NH₄F]-13d showed small amounts of anatase-like TiO₂ as indicated by the presence of a 330-nm band. Prolonging the crystallization period from seven to 13 days, the intensity of the 210-nm band related to the framework Ti increased greatly as compared Ti-CFI[HF]-seed-7d and Ti-CFI[HF]-seed-13d, which was consistent with the results of the ICP test (Table 1). As indicated in the Figure 3B, the sample Ti-CFI[LiOH] synthesized in the LiOH system without post-treatment processes showed the main absorbance band at about 250 nm, indexed as extra-framework Ti species. After post-treatment with acid, the sample Ti-CFI[LiOH]-post only displayed absorbance at about 210 nm, indexed as framework Ti species; however, the intensity decreased greatly.

Table 1. Product yields, chemical compositions, and porosity properties of Ti-CFI zeolites from the different synthetic systems.

Samples	Yields (%)	Si/Ti (mol/mol)	S _{BET} ¹ (m ² ·g ⁻¹)	Pore Volume (m ³ ·g ⁻¹)	S _{ext.} ² (m ² ·g ⁻¹)
Ti-CFI[HF]-seed-7d	~90	247	395	0.14	33
Ti-CFI[HF]-seed-13d	~90	189	413	0.15	36
Ti-CFI[NH ₄ F]-13d	~92	220	385	0.14	22
Ti-CFI[LiOH]	~85	46	280	0.08	84
Ti-CFI[LiOH]-post	-	183	393	0.11	101

¹ Brunauer–Emmett–Teller (BET) specific surface area. ² External specific surface areas were calculated from the t-plot curve.

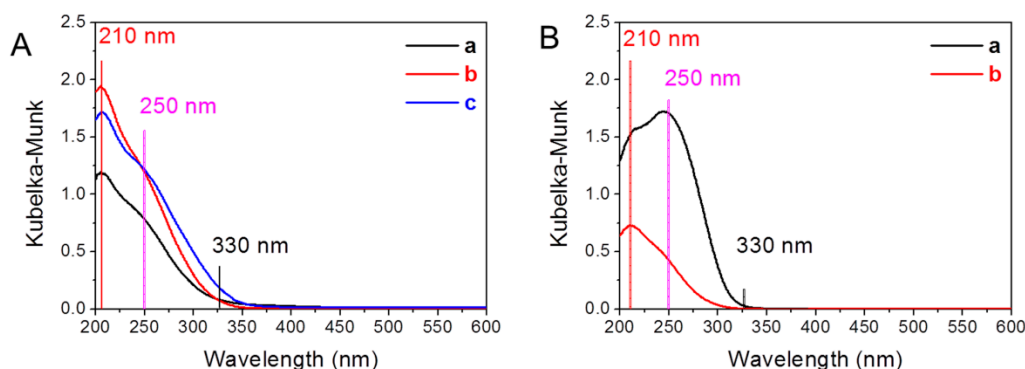


Figure 3. Diffuse reflectance ultraviolet/visible light (DRUV/Vis) spectra of Ti-CFI extra-large-pore zeolites synthesized in fluoride system (A): (a) Ti-CFI[HF]-seed-7d, (b) Ti-CFI[HF]-seed-13d, and (c) Ti-CFI[NH₄F]-13d, and synthesized in LiOH system (B): (a) Ti-CFI[LiOH] and (b) Ti-CFI[LiOH]-post.

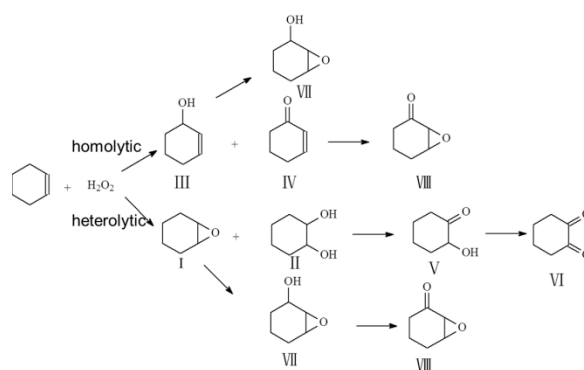
2.2. Catalytic Tests

The characterization showed that well-crystallized Ti-CFI zeolites with framework titanium species could be synthesized in the HF system with seed or in the NH₄F system without seed. Here, catalytic oxidation of cyclohexene using H₂O₂ as an oxidant was employed to test their catalytic performance, while the samples synthesized in the LiOH system were used as controls. Table 2 shows the results of epoxidation of cyclohexene. The reaction routes are shown in Scheme 1. The cyclohexene oxide (I), generated by the heterolytic epoxidation of the cyclohexene C=C double bond, and the 1,2-cyclohexanediol (II) side product, formed by hydrolysis of epoxide ring, generally reflect a concerted process. In contrast, the allylic oxidation side products, 2-cyclohexen-1-ol (III) and 2-cyclohexen-1-one (IV), are often ascribed to a homolytic radical pathway [28]. Others including V, VI, VII, and VIII are the products of further oxidation.

Table 2. Catalytic oxidation of cyclohexene over various Ti-CFI zeolites using H₂O₂ aqueous solution as an oxidant.

Samples	Si/Ti (mol/mol)	Conversion (%)	Selectivity (%)					TON (mol/mol -Ti)	H ₂ O ₂ Efficiency ¹ (%)
			I	II	III	IV	Others		
Ti-CFI[HF]-seed-7d	247	8.2	17.0	68.9	4.2	6.1	3.8	49	>99
Ti-CFI[HF]-seed-13d	189	9.0	14.7	69.9	4.6	4.5	11.9	41	>99
Ti-CFI[NH ₄ F]-13d	220	5.3	8.7	74.8	4.3	6.9	5.3	28	>99
Ti-CFI[LiOH]	46	2.0	73.9	14.9	4.2	4.3	2.7	2	12
Ti-CFI[LiOH]-post	183	4.8	14.1	62.3	11.9	4.5	7.2	21	34

$$^1 \text{H}_2\text{O}_2 \text{ utilization efficiency \%} = (\text{I} + \text{II} + \text{III} + \text{IV} \times 2 + (\text{others}) \times 2) / \text{converted H}_2\text{O}_2 \times 100.$$



Scheme 1. The possible reaction routes for oxidation of cyclohexene with H₂O₂ as an oxidant.

Table 2 shows the results of catalytic oxidation of cyclohexene over Ti-CFI zeolites using H₂O₂ aqueous solution as an oxidant. Ti-CFI[LiOH] from the LiOH system showed extremely low

catalytic activity, as indicated by the low cyclohexene conversion and low turnover numbers (TON). The catalytic activity was increased after post-treatment to remove extra-framework Ti species. Significantly, all the Ti-CFI synthesized with fluorides showed high cyclohexene conversion, TON and higher H₂O₂ utilization efficiency than those of samples synthesized with LiOH. Moreover, comparing Ti-CFI[NH₄F]-13d with Ti-CFI[LiOH]-post, they had similar cyclohexene conversions; however, sample Ti-CFI[NH₄F]-13d from the fluoride system generated more heterolytic products of I and II. Comparing samples of Ti-CFI[HF]-seed-13d and Ti-CFI[NH₄F]-13d, sample Ti-CFI[HF]-seed-13d showed higher catalytic performance than that of Ti-CFI[NH₄F]-13d. The higher catalytic performance was attributed to higher Ti content, small crystal size, and higher micropore volume, which was consistent with the above results from DRUV/Vis spectra, nitrogen adsorption analysis, and SEM characterizations.

3. Materials and Methods

3.1. Synthesis of Titanium-Containing CFI-Type Extra-Large-Pore Zeolites in the Fluoride System

The Ti-CFI zeolites were synthesized under hydrothermal conditions in a rotating Teflon-lined autoclave (50 revolutions per minute) at 448 K for 7–13 days from the following composition: 1 SiO₂/0.01 TiO₂/0.5 N(16)-methylsperineium hydroxide/0.5 HF (NH₄F)/5–15 H₂O/0.1 H₂O₂. In a typical run, titanium tetra-*n*-butoxide was added to an H₂O₂ aqueous solution to form a stable Ti source of Ti-peroxo complexes, which were added into an aqueous solution of N(16)-methylsperineium hydroxide. Then, tetraethylorthosilicate was added into the above mixture under stirring. After stirring for 30 minutes, the resultant solution was heated to 353 K to evaporate the alcohol generated during the hydrolysis of the Ti and Si precursors. After completely evaporating the alcohol, the mixture was cooled down, and HF or NH₄F was carefully dropped. Then, 5 wt.% seeds of pure silica CFI zeolite synthesized as reported [29] in the presence of fluoride were added if required. The final mixture was transferred into an autoclave and treated at 448 K under rotation. The solid product was centrifuged, washed with distilled water, and dried at 373 K, before being calcined at 823 K for 6 h to remove the organic templates. The obtained Ti-CFI zeolites using HF and NH₄F as fluoride sources were denoted as Ti-CFI[HF]-*x*d and Ti-CFI[NH₄F]-*x*d, respectively, where *x* represents the time of hydrothermal synthesis. The obtained Ti-CFI zeolites upon adding seeds were denoted as Ti-CFI[HF]-seed.

3.2. Synthesis of Titanium-Containing CFI-Type Extra-Large-Pore Zeolites in the LiOH System

In a typical run, titanium tetra-*n*-butoxide was added to an H₂O₂ aqueous solution to form a stable Ti source of Ti-peroxo complexes, which were added into an aqueous solution of N(16)-methylsperineium hydroxide. Then tetraethylorthosilicate was added into above mixture under stirring. After stirring for 30 minutes, the resultant solution was heated to 353 K to evaporate the alcohol generated during the hydrolysis of the Ti and Si precursors. After completely evaporating the alcohol, the clear solution was cooled down, and LiOH was added. The final mixture with the composition of 0.05 Li₂O/1 SiO₂/0.02 TiO₂/0.3 N(16)-methylsperineium hydroxide/40 H₂O/0.1 H₂O₂ was transferred into an autoclave and treated at 423 K under rotation for 10 days. The solid product was centrifuged, washed with distilled water, dried at 373 K, and calcined at 823 K for 6 h to remove the organic templates. The obtained sample was denoted as Ti-CFI[LiOH]. If the sample was further treated by washing with 1.0 M HCl at room temperature for 24 hours to remove the extra-framework Ti species, the obtained Ti-CFI zeolites were denoted as Ti-CFI[LiOH]-post.

3.3. Catalytic Reaction

Epoxidation reactions were performed in a 10-mL glass reactor immersed in a 60 °C oil bath, using H₂O₂ (35 wt.% in water) as an oxidant. In a typical run, the reactions were carried out with 25 mg of catalyst, 1.0 mmol of cyclohexene, and 1.0 mmol of H₂O₂ in 2.0 mL of acetonitrile with vigorous stirring for 4 h. Reaction mixtures were analyzed by gas chromatography (GC) using a Shimadzu GC-2014 (Kyoto, Japan) equipped with a 60-m TC-1 capillary column and a flame ionization

detector (FID). The amount of the unconverted H_2O_2 was determined by titrating with 0.1 M $\text{Ce}(\text{SO}_4)_2$ aqueous solution. The products were verified using authentic chemicals commercially available.

3.4. Characterization

Powder X-ray diffraction (PXRD) patterns were measured by a Rigaku Ultima III instrument (Beijing, China) equipped with a $\text{Cu-K}\alpha$ X-ray source (40 kV and 20 mA). Nitrogen adsorption–desorption measurements were measured at 77 K on a BELSORP-Mini II, (MicrotracBEL Corp., Osaka, Japan). Microporous volume and external surface area were calculated from *t*-plot curves. Field-emission scanning electron microscope (SEM) images were obtained on a Hitachi S-5200 microscope (Tokyo, Japan) operated at 1 kV and 10 μA . The content of Si and Ti was tested on a Shimadzu ICPE-9000 (Kyoto, Japan) inductively coupled plasma-atomic emission spectrometer (ICP). Diffuse reflectance UV/Vis spectra (DRUV/Vis) were recorded on a V-650DS spectrophotometer (JASCO, Tokyo, Japan). The diffuse reflectance spectra were converted into the absorption spectra using the Kubelka–Munk function.

4. Conclusions

Ti-containing CFI-type extra-large-pore zeolites were directly synthesized in a fluoride system. The addition of a seed could accelerate the crystallization process and decrease the crystal size. Prolonging the crystallization process could increase the Ti content and pore volume, which was beneficial to the catalytic performance. Compared with the Ti-CFI sample synthesized in the LiOH system, Ti-CFI synthesized in the presence of fluorides showed higher catalytic performance and higher H_2O_2 utilization efficiency. This indicated that the fluoride synthetic system was a good synthetic system for the synthesis of Ti-containing CFI-type extra-large-pore zeolites, which could be extended to the synthesis of other types of Ti-containing zeolites.

Supplementary Materials: The following are available online at <http://www.mdpi.com/2073-4344/9/3/257/s1>: Figure S1: (A) PXRD and (B) SEM image of the pure silica CFI-type zeolite synthesized in the HF system, which was used as a seed for the preparation of Ti-CFI; Figure S2: SEM image of as-synthesized Ti-CFI[LiOH].

Author Contributions: Conceptualization, J.-G.W. and T.L.; material preparation, Y.W. and Y.S.; synthesis and data analysis, Y.W., H.W., and J.-G.W.; writing—original draft, Y.W. and J.-G.W.; writing—review and editing, Y.W., H.W., Y.S., T.L., T.T., and J.-G.W.; funding acquisition, T.L., and J.-G.W. All authors gave approval for the final version of the manuscript.

Funding: This research was funded by the National Natural Science Foundation of China, grant numbers 51602164 and 21776143, the Program for Scientific Research Innovation Team in Colleges and Universities of Shandong Province, and the Japan Society for the Promotion of Science (JSPS) fellowship.

Conflicts of Interest: The authors declare no conflicts of interest.

References

1. Martinez, C.; Corma, A. Inorganic molecular sieves: Preparation, modification and industrial application in catalytic processes. *Coord. Chem. Rev.* **2011**, *255*, 1558–1580. [[CrossRef](#)]
2. Choi, M.; Na, K.; Kim, J.; Sakamoto, Y.; Terasaki, O.; Ryoo, R. Stable single-unit-cell nanosheets of zeolite MFI as active and long-lived catalysts. *Nature* **2009**, *461*, 246–249. [[CrossRef](#)] [[PubMed](#)]
3. Zhang, X.; Liu, D.; Xu, D.; Asahina, S.; Cychoz, K.A.; Agrawal, K.V.; Al Wahedi, Y.; Bhan, A.; Al Hashimi, S.; Terasaki, O.; et al. Synthesis of self-pillared zeolite nanosheets by repetitive branching. *Science* **2012**, *336*, 41. [[CrossRef](#)]
4. Ding, K.; Corma, A.; Macia-Agullo, J.A.; Hu, J.G.; Kramer, S.; Stair, P.C.; Stucky, G.D. Constructing Hierarchical Porous Zeolites via Kinetic Regulation. *J. Am. Chem. Soc.* **2015**, *137*, 11238–11241. [[CrossRef](#)]
5. Feng, G.; Cheng, P.; Yan, W.; Boronat, M.; Li, X.; Su, J.H.; Wang, J.; Li, Y.; Corma, A.; Xu, R.; et al. Accelerated crystallization of zeolites via hydroxyl free radicals. *Science* **2016**, *351*, 1188–1191. [[CrossRef](#)] [[PubMed](#)]
6. Prech, J.; Pizarro, P.; Serrano, D.P.; Cejka, J. From 3D to 2D zeolite catalytic materials. *Chem. Soc. Rev.* **2018**, *47*, 8263–8306. [[CrossRef](#)] [[PubMed](#)]

7. Taramasso, M.; Perego, G.; Notari, B. Preparation of porous crystalline synthetic material comprised of silicon and titanium oxides. U.S. Patent 4,410,501, 18 October 1983.
8. Lin, M.; Xia, C.; Zhu, B.; Li, H.; Shu, X. Green and efficient epoxidation of propylene with hydrogen peroxide (HPPO process) catalyzed by hollow TS-1 zeolite: A 1.0 kt/a pilot-scale study. *Chem. Eng. J.* **2016**, *295*, 370–375. [[CrossRef](#)]
9. Wang, J.G.; Wang, Y.B.; Tatsumi, T.; Zhao, Y.L. Anionic polymer as a quasi-neutral medium for low-cost synthesis of titanosilicate molecular sieves in the presence of high-concentration alkali metal ions. *J. Catal.* **2016**, *338*, 321–328. [[CrossRef](#)]
10. Zhao, H.; Yokoi, T.; Kondo, J.N.; Tatsumi, T. Hydrophobicity enhancement of Ti-MWW catalyst and its improvement in oxidation activity. *Appl. Catal. A-Gen.* **2015**, *503*, 156–164. [[CrossRef](#)]
11. Zhao, S.; Xie, W.; Liu, Y.; Wu, P. Methyl Ethyl Ketone Ammoximation over Ti-MWW in a Continuous Slurry Reactor. *Chinese J. Catal.* **2011**, *32*, 179–183. [[CrossRef](#)]
12. Reddy, J.S.; Kumar, R.; Ratnasamy, P. ChemInform Abstract: Titanium Silicalite-2: Synthesis, Characterization, and Catalytic Properties. *Appl. Catal.* **1990**, *58*, L1–L4. [[CrossRef](#)]
13. Serrano, D.P.; Li, H.X.; Davis, M.E. Synthesis of titanium-containing ZSM-48. *J. Chem. Soc. Chem. Commun.* **1992**, *10*, 745–747. [[CrossRef](#)]
14. Wu, P.; Tatsumi, T.; Komatsu, T.; Yashima, T. A novel titanosilicate with MWW structure. I. Hydrothermal synthesis, elimination of extraframework titanium, and characterizations. *J. Phys. Chem. B* **2001**, *105*, 2897–2905. [[CrossRef](#)]
15. Cambor, M.A.; Corma, A.; Martínez, A.; Pérez-Pariente, J. Synthesis of a titaniumsilicoaluminate isomorphous to zeolite beta and its application as a catalyst for the selective oxidation of large organic molecules. *J. Chem. Soc. Chem. Commun.* **1992**, 589–590. [[CrossRef](#)]
16. Blasco, T.; Cambor, M.; Corma, A.; Esteve, P.; Guil, J.; Martínez, A.; Perdigon-Melon, J.; Valencia, S. Direct synthesis and characterization of hydrophobic Aluminum-free Ti-beta zeolite. *J. Phys. Chem. B* **1998**, *102*, 75–88. [[CrossRef](#)]
17. Van der Waal, J.; Kooyman, P.; Jansen, J.; Van Bekkum, H. Synthesis and characterization of aluminum-free zeolite titanium beta using di (cyclohexylmethyl) dimethylammonium as a new and selective template. *Micropor. Mesopor. Mater.* **1998**, *25*, 43–57. [[CrossRef](#)]
18. Tuel, A. Synthesis, characterization, and catalytic properties of the new TiZSM-12 zeolite. *Zeolites* **1995**, *15*, 236–242. [[CrossRef](#)]
19. Wu, P.; Komatsu, T.; Yashima, T. Characterization of titanium species incorporated into dealuminated mordenites by means of IR spectroscopy and 18O-exchange technique. *J. Phys. Chem.* **1996**, *100*, 10316–10322. [[CrossRef](#)]
20. Díaz-Cabañas, M.-J.; Villaescusa, L.A.; Cambor, M.A. Synthesis and catalytic activity of Ti-ITQ-7: a new oxidation catalyst with a three-dimensional system of large pore channels. *Chem. Commun.* **2000**, 761–762. [[CrossRef](#)]
21. Fan, W.; Wu, P.; Namba, S.; Tatsumi, T. A titanosilicate that is structurally analogous to an MWW-type lamellar precursor. *Angew. Chem. Int. Ed.* **2004**, *43*, 236–240. [[CrossRef](#)]
22. Tamura, M.; Chaikittisilp, W.; Yokoi, T.; Okubo, T. Incorporation process of Ti species into the framework of MFI type zeolite. *Microporous Mesoporous Mater.* **2008**, *112*, 202–210. [[CrossRef](#)]
23. Wang, J.G.; Yokoi, T.; Kondo, J.N.; Tatsumi, T.; Zhao, Y.L. Titanium(IV) in the Organic-Structure-Directing-Agent-Free Synthesis of Hydrophobic and Large-Pore Molecular Sieves as Redox Catalysts. *ChemSuschem* **2015**, *8*, 2476–2480. [[CrossRef](#)]
24. Luna, F.J.; Ukawa, S.E.; Wallau, M.; Schuchardt, U. Cyclohexane oxidation using transition metal-containing aluminophosphates (MAPO-VFI). *J. Mol. Catal. A-Chem.* **1997**, *117*, 405–411. [[CrossRef](#)]
25. Prech, J.; Čejka, J. UTL titanosilicate: An extra-large pore epoxidation catalyst with tunable textural properties. *Catal. Today* **2016**, *277*, 2–8. [[CrossRef](#)]
26. Balkus, K., Jr.; Gabrielov, A.; Zones, S. The synthesis of UTD-1, Ti-UTD-1 and Ti-UTD-8 using CP* 2CoOH as a structure directing agent. *Stud. Surf. Sci. Catal.* **1995**, *97*, 519–525.
27. Prech, J.; Kubů, M.; Čejka, J. Synthesis and catalytic properties of titanium containing extra-large pore zeolite CIT-5. *Catal. Today* **2014**, *227*, 80–86. [[CrossRef](#)]

28. Sever, R.R.; Alcala, R.; Dumesic, J.A.; Root, T.W. Vapor-phase silylation of MCM-41 and Ti-MCM-41. *Micropor. Mesopor. Mater.* **2003**, *66*, 53–67. [[CrossRef](#)]
29. Barrett, P.A.; Díaz-Cabañas, M.J.; Cambor, M.A.; Jones, R.H. Synthesis in fluoride and hydroxide media and structure of the extra-large pore pure silica zeolite CIT-5. *J. Chem. Soc. Faraday Trans.* **1998**, *94*, 2475–2481. [[CrossRef](#)]



© 2019 by the authors. Licensee MDPI, Basel, Switzerland. This article is an open access article distributed under the terms and conditions of the Creative Commons Attribution (CC BY) license (<http://creativecommons.org/licenses/by/4.0/>).